

Accelerated Variance Reduced Block Coordinate Descent

Zebang Shen, Hui Qian, Chao Zhang, and Tengfei Zhou
 {shenzebang,qianhui,zczju,zhoutengfei_zju@zju.edu.cn}
 Zhejiang University

September 18, 2017

Abstract

Algorithms with fast convergence, small number of data access, and low per-iteration complexity are particularly favorable in the big data era, due to the demand for obtaining *highly accurate solutions* to problems with *a large number of samples* in *ultra-high* dimensional space. Existing algorithms lack at least one of these qualities, and thus are inefficient in handling such big data challenge. In this paper, we propose a method enjoying all these merits with an accelerated convergence rate $\mathcal{O}(\frac{1}{k^2})$. Empirical studies on large scale datasets with more than one million features are conducted to show the effectiveness of our methods in practice.

Introduction

In this paper, we consider the minimization of smooth convex function with non-smooth convex regularization:

$$\min_{\mathbf{x} \in \mathbb{R}^d} \mathbf{F}^{\mathbf{P}}(\mathbf{x}) = \mathbf{F}(\mathbf{x}) + \mathbf{P}(\mathbf{x}), \quad (1)$$

where $\mathbf{F}(\mathbf{x}) = \frac{1}{n} \sum_{i=1}^n f_i(\mathbf{x})$ is the average of n smooth convex component functions f_i 's and $\mathbf{P}(\mathbf{x})$ is the possibly non-smooth convex regularization term. Many machine learning problems can be phrased as the above problem.

However, the explosive growth of data poses two challenges to solving the aforementioned problem: (i) the number of samples can easily reach the magnitude of millions, and (ii) the dimensionality of these massive datasets is ultra-high in the meantime. Fast converging algorithms that meet these challenges have been ardently pursued in the recent years.

To solve optimization problems with enormous samples, the classical Stochastic Gradient Descent (SGD) has gained increasing attention in the last decade. The advantage of such methods is that only one sample is access in each iteration. While the vanilla version inherently suffers from the slow convergence rate due to the stochastic nature of SGD, one of its variant, named Stochastic Variance Reduced Gradient

(SVRG) [9], proposes to mix the exact full gradient and stochastic gradient in a way that better convergence results can be obtained without compromising the low per-iteration sample access [11, 15]. Works based on such Variance Reduction (VR) technique have proliferated in the past few years. For example, [19] extends SVRG to an asynchronous setting so that the parallelism in modern computational architecture can be fully utilized and [3] improves the convergence of SVRG in non-strongly convex case and provides a convergence result in non-convex case. Besides, there are also alternatives to SVRG, such as SAG [22] and SAGA [4]. Attempts are made to accelerate the convergence of SGD type methods, e.g. [26, 7, 13, 1, 8] and the newly proposed Katyusha [1], which is the first direct accelerated version of SVRG. However, since SGD type methods perform full vector operation in each iteration, they are precluded to handle problems in high dimension.

To deal with the ultra-high dimensionality in sparse learning tasks, Coordinate Descent (CD) type methods were given a renewed interest in the past few years. The basic idea of Coordinate Descent (CD) type methods is that, in each iteration, approximate the problem with respect to some components of the variable \mathbf{x} while keeping the rest unchanged [23]. With such technique, full vector operations are avoided, making low per-iteration complexity possible. Randomness is also incorporated into CD type methods [16, 20], with which convergence results are readily obtained. There has been some recent works on CD that introduce non-uniform sampling [17, 18, 2], and consider the asynchronous [14] and distributed settings [21] for better scalability. Accelerated versions of CD type methods have also emerged, for example APPROX [5] gives practical implementation and is applicable to general convex optimization problem. A drawback of CD type methods is that all samples are accessed in each iteration. When the number of samples is huge, they can still be quite slow.

As discussed above, existing algorithms only handle problems with either small n or small d . There has been two exceptions MRBCD [27] and S2CD [10], which however have no accelerated version and thus can be further improved. In this work, we propose a method called Accelerated Variance Reduced Block Coordinate Descent (AVRBCD) that tackles the two challenges in large scale problem. We show that our method enjoys a superior convergence rate. Specifically, the advantages of AVRBCD are listed as follows.

1. VR technique is used in AVRBCD, and it accesses only one sample per-iteration in amortized analysis,
2. AVRBCD avoids full vector operation in each iteration, and is shown to have low per-iteration complexity in solving sparse Empirical Risk Minimization problem,
3. AVRBCD is an accelerated version of MRBCD, with convergence rate $\mathcal{O}(\frac{1}{k^2})$, compared to $\mathcal{O}(\frac{1}{k})$ in MRBCD.

To show the effectiveness of AVRBCD in practice, we conduct several experiments on datasets with both large n and large p . One of our experiment has more than one million variables ($d > 10^6$). The experiments on the real-word datasets demonstrate superior computational efficiency of our approaches compared to the state of the arts.

Preliminary

In this section, we give the notations and assumptions used in this paper. The VR, CD, and accelerating techniques are discussed. We also introduce the Empirical Risk Minimization (ERM) problem with linear predictor.

Notation & Assumptions

We assume that the variable $\mathbf{x} \in \mathbb{R}^d$ is partitioned into B blocks and B divides d for simplicity. Let $\Omega = \frac{d}{B}$ be the block size. The regularization $\mathbf{P}(\mathbf{x})$ is assumed to be separable with respect to the partition of \mathbf{x} , i.e.

$$\mathbf{P}(\mathbf{x}) = \sum_{l=1}^B \mathbf{P}_l([\mathbf{x}]_l), \quad (2)$$

where $[\mathbf{x}]_l \in \mathbb{R}^\Omega$ corresponds to the l^{th} block of \mathbf{x} . We shall use $[\mathbf{x}]_{\setminus l}$ to denote the blocks of \mathbf{x} other than the l^{th} . Such assumption stands for many important functions, e.g. the sparse inducing l_1 norm $\|\cdot\|_1$. The proximal operator of a convex function g is defined as

$$\text{prox}_g(\mathbf{y}) = \underset{\mathbf{x}}{\text{argmin}} g(\mathbf{x}) + \frac{1}{2}\|\mathbf{x} - \mathbf{y}\|^2, \quad (3)$$

where we use $\|\cdot\|$ to denote the Euclidean norm. We say a function f is L -smooth, if for any \mathbf{x} and \mathbf{y} ,

$$f(\mathbf{y}) \leq f(\mathbf{x}) + \langle \nabla f(\mathbf{x}), \mathbf{y} - \mathbf{x} \rangle + \frac{L}{2}\|\mathbf{x} - \mathbf{y}\|^2. \quad (4)$$

Each component function is assumed to be f_i is L_i -smooth, with $L_{max} = \max L_i$. We also assume that their average \mathbf{F} is L_l -smooth with respect to the l^{th} block and define $L_B = \max L_l$. Finally, we define $\tilde{L} = \max\{BL_B, L_{max}\}$.

Variance Reduction

SGD uses the gradient of a randomly chosen component function f_i as an unbiased estimator of the exact full gradient $\nabla \mathbf{F}(\mathbf{x}_k)$. The variance introduced by such randomness forces a diminishing step size and leads to slow convergence rate, e.g. $\mathcal{O}(\frac{1}{\sqrt{k}})$ for smooth convex minimization. [9] proposes to keep the full gradient $\nabla \mathbf{F}(\tilde{\mathbf{x}})$ at some snapshot $\tilde{\mathbf{x}}$ and constructs a mixed gradient as

$$\mathbf{v}_k = \nabla f_i(\mathbf{x}_k) - \nabla f_i(\tilde{\mathbf{x}}) + \nabla \mathbf{F}(\tilde{\mathbf{x}}). \quad (5)$$

They show that the variance of \mathbf{v}_k , i.e. $\|\mathbf{v}_k - \nabla \mathbf{F}(\mathbf{x}_k)\|$, converges to zero when both \mathbf{x}_k and $\tilde{\mathbf{x}}$ converge to the optimal point \mathbf{x}^* . For smooth convex minimization, the best known convergence result of SVRG is $\mathcal{O}(\frac{1}{k})$ due to [3]. Besides, in doing so, SVRG only accesses one sample per iteration in amortized analysis, making it ideal when only the number of samples n is large. However, since full vector operation is need in each iteration of such algorithm, SVRG can still be inefficient when the dimensionality d of the problem is ultra-high.

Randomized Block Coordinate Descent (RBCD)

RBCD extends Randomized CD such that a block of coordinates rather than only one coordinate can be updated in each iteration. More specifically, the update rule writes

$$[\mathbf{x}_k]_l = [\mathbf{x}_{k-1}]_l - \eta[\nabla\mathbf{F}(\mathbf{x}_{k-1})]_l, [\mathbf{x}_k]_{\setminus l} = [\mathbf{x}_{k-1}]_{\setminus l}, \quad (6)$$

where l is the coordinate block randomly selected in the k^{th} iteration and η is some step size. RBCD also bridges CD and Gradient Descent (GD). It becomes CD when the block size Ω is set to 1 and when Ω is set to d , it becomes GD. The convergence rate of RBCD is $\mathcal{O}(\frac{B}{k})$ [16] which is B times worse than that of GD. But in applications like sparse ERM problems discussed below, the per-iteration complexity of RBCD can be decreased to $\mathcal{O}(\frac{d}{B})$, when B is appropriately chosen. So CD has the same overall complexity as GD but with a much smaller per-iteration complexity, which is suitable for problems in ultra-high dimensional space. However, one major flaw about RBCD is that it accesses all n component functions in each iteration. When n is large, RBCD can still be slow.

APPROX & Katyusha

Accelerated versions have been proposed for SVRG and RBCD, namely Katyusha [1] and APPROX [5] respectively. Both algorithms utilized the momentum to speed up the convergence. In Katyusha, the authors use the snapshot $\tilde{\mathbf{x}}$ as an additional "negative momentum" to overcome the difficulty in handling noisy stochastic gradient. In APPROX, as originally discussed in [16], although the convergence is relatively easy to prove, a naive implementation would still involve full vector operation in each iteration. The authors took the transformation technique proposed in [12] and derived an equivalent alternative to avoid such issue. Both Katyusha and APPROX can be taken as special case of AVRBCD. Indeed, when we take $\Omega = d$, AVRBCD degenerates to Katyusha (with opt. II), and when we take $m = 1$ and $\alpha_{3,s} = 0$, AVRBCD becomes APPROX.

Empirical Risk Minimization

We give a brief introduction to an important class of smooth convex problems, the Empirical Risk Minimization (ERM) with linear predictor. It will be used when analyzing the per-iteration complexity of AVRBCD. Specifically, we assume each $f_i(\cdot)$ is of the form $f_i(\mathbf{x}) = \phi_i(\mathbf{a}_i^\top \mathbf{x})$, where \mathbf{a}_i is the feature vector of the i^{th} sample and $\phi_i(\cdot) : \mathbb{R} \rightarrow \mathbb{R}$ is some smooth convex loss function. $\mathbf{A} = [\mathbf{a}_1 \dots \mathbf{a}_n]^\top$ is the data matrix. In real applications, \mathbf{A} is usually very sparse and we define to be the sparsity of \mathbf{A}

$$\rho = \frac{nnz(\mathbf{A})}{nd}. \quad (7)$$

For simplicity, we assume the zeros in \mathbf{A} are shattered uniformly.

Algorithm 1 AVRBCD I

Input: $m, \mathbf{x}_0, \alpha_{1,0}, \alpha_{2,0}$

- 1: $\mathbf{z}_0 \leftarrow \mathbf{x}_0, \tilde{\mathbf{x}}^0 \leftarrow \mathbf{x}_0;$
 - 2: **for** $s \leftarrow 0$ **to** S **do**
 - 3: $\alpha_{2,s} = \frac{\sqrt{\alpha_{2,s-1}^4 + 4\alpha_{2,s-1}^2 - \alpha_{2,s-1}^2}}{2};$
 - 4: $\alpha_{1,s} = \alpha_{1,s-1}(1 - \alpha_{2,s}), \alpha_{3,s} = 1 - \alpha_{1,s} - \alpha_{2,s};$
 - 5: $\bar{L}_s = \frac{L_Q}{B\alpha_{3,s}} + L_B, \eta_s = \frac{1}{L_s\alpha_{2,s}B};$
 - 6: $\mu^s = \nabla f(\tilde{\mathbf{x}}^s);$
 - 7: **for** $j \leftarrow 1$ **to** m **do**
 - 8: $k \leftarrow (sm) + j;$
 - 9: $\mathbf{y}_k = \alpha_{1,s}\mathbf{x}_{k-1} + \alpha_{2,s}\mathbf{z}_{k-1} + \alpha_{3,s}\tilde{\mathbf{x}}^s;$
 - 10: **sample** i **from** $\{1, \dots, n\}$ **and** l **from** $\{1, \dots, B\};$
 - 11: $\mathbf{v}_k = \mu^s + \nabla f_i(\mathbf{y}_k) - \nabla f_i(\tilde{\mathbf{x}}^s);$
 - 12: $[\mathbf{z}_k]_l = \text{prox}_{\eta_s \mathbf{P}_i}([\mathbf{z}_{k-1} - \eta_s \mathbf{v}_k]_l);$
 - 13: $[\mathbf{z}_k]_{\setminus l} = [\mathbf{z}_{k-1}]_{\setminus l};$
 - 14: $\mathbf{x}_k = \mathbf{y}_k + \alpha_{2,s}B(\mathbf{z}_k - \mathbf{z}_{k-1});$
 - 15: **end for**
 - 16: **Sample** σ_s **from** $\{1, \dots, m\}$ **uniformly;**
 - 17: $\tilde{\mathbf{x}}^{s+1} = \mathbf{x}_{sm+\sigma_s};$
 - 18: **end for**
-

Methodology

In this section, we present the proposed algorithm AVRBCD in two different but equivalent forms listed in Algorithm 1 and 2. The former is easier to analyze and latter is of more practical interest as it has smaller per-iteration complexity.

AVRBCD

We divide our algorithm into epochs, at the beginning of which the full gradient in some snapshot $\tilde{\mathbf{x}}^s$ is computed. As a mixture of (5) and (6), m updating steps are taken in the follow-up inner loops. Different from MRBCD, two additional coupling steps are added to ensure the acceleration of our method: line 9 uses the two momentum technique proposed by [1], and line 14 is a common practice in accelerated methods such as [16, 5]. Note that we write line 11 just for ease of notation and only $[\mathbf{v}_k]_l$ is needed in practice. We will show that AVRBCD enjoys the accelerated convergence rate in the next section.

Implementation without Full Vector Operation

Similar to the methods in [16, 12, 5], AVRBCD I requires $\mathcal{O}(d)$ computation in each inner loop due to the convex combination in line 9, which invalidates the advantage of low per-iteration complexity in BCD type methods. Borrowing ideas from [12, 5], we propose a more practical implementation of AVRBCD in Algorithm 2, avoiding the full

vector operation in the inner loop. Three functions $\{\bar{\mathbf{x}}_k, \bar{\mathbf{y}}_k, \bar{\mathbf{z}}_k\}$ are used in AVRBCD II and we give their definitions here

$$\bar{\mathbf{y}}_k = \beta_{j-1} \mathbf{u}_{j-1}^s + \gamma_s \hat{\mathbf{z}}_{j-1}^s + \dot{\mathbf{x}}^s, \quad (8)$$

$$\bar{\mathbf{z}}_k = \hat{\mathbf{z}}_j^s + \dot{\mathbf{x}}^s, \quad (9)$$

$$\bar{\mathbf{x}}_k = \beta_{j-1} \mathbf{u}_j^s + \gamma_s \hat{\mathbf{z}}_j^s + \dot{\mathbf{x}}^s, \quad (10)$$

with $k = sm + j$. In order to see the equivalence between Algorithm 1 and 2, we give the following proposition.

Proposition 1. $\bar{\mathbf{x}}_k = \mathbf{x}_k$, $\bar{\mathbf{y}}_k = \mathbf{y}_k$, and $\bar{\mathbf{z}}_k = \mathbf{z}_k$ hold for all k , if $\bar{i}_k = i_k$, $\bar{l}_k = l_k$, and $\sigma_s = \bar{\sigma}_s$ for all k and s , where \mathbf{x}_k , \mathbf{y}_k , \mathbf{z}_k , i_k , and l_k are in Algorithm 1, and $\bar{\mathbf{x}}_k$, $\bar{\mathbf{y}}_k$, $\bar{\mathbf{z}}_k$, \bar{i}_k , \bar{l}_k , and $\bar{\sigma}_s$ are defined in (8), (9), (10), and Algorithm 2.

Proof. First, we prove that if at the beginning of the s^{th} epoch, i.e. $j = 0$ and $k = sm$, $\bar{\mathbf{z}}_k = \mathbf{z}_k$ and $\bar{\mathbf{x}}_k = \mathbf{x}_k$ stand, then all these three equations stand in the following iterations in that epoch. We prove with induction. Assume that the equivalence holds up till the $\kappa - 1^{th}$ iteration. Since $\sigma_s = \bar{\sigma}_s$, we have $\tilde{\mathbf{x}}^s = \dot{\mathbf{x}}^s$. In the κ^{th} iteration, for $\bar{\mathbf{y}}_\kappa$ we have

$$\begin{aligned} \mathbf{y}_\kappa &= \alpha_{1,s} \bar{\mathbf{x}}_{\kappa-1} + \alpha_{2,s} \bar{\mathbf{z}}_{\kappa-1} + \alpha_{3,s} \dot{\mathbf{x}}^s \\ &= \alpha_{1,s} (\beta_{j-2}^s \mathbf{u}_{j-1}^s + \gamma_s \hat{\mathbf{z}}_{j-1}^s) + \alpha_{2,s} \hat{\mathbf{z}}_{j-1}^s + \dot{\mathbf{x}}^s \\ &= \beta_{j-1}^s \mathbf{u}_{j-1}^s + \gamma_s \hat{\mathbf{z}}_{j-1}^s + \dot{\mathbf{x}}^s = \bar{\mathbf{y}}_\kappa. \end{aligned}$$

since $\alpha_{1,s} \beta_{j-2}^s = \beta_{j-1}^s$ and $\alpha_{1,s} \gamma_s + \alpha_{2,s} = \gamma_s$. Suppose the l^{th} block is selected in that section, by induction we have

$$[\bar{\mathbf{z}}_\kappa]_{\setminus l} = [\mathbf{z}_{\kappa-1}]_{\setminus l} = [\mathbf{z}_\kappa]_{\setminus l}$$

and

$$\begin{aligned} [\bar{\mathbf{z}}_\kappa]_l &= [\mathbf{z}_j^s + \dot{\mathbf{x}}^s]_l = \text{prox}_{\eta \mathbf{P}_l}([\hat{\mathbf{z}}_{j-1}^s + \dot{\mathbf{x}}^s - \eta \tilde{\nabla}_\kappa]_l) \\ &= \text{prox}_{\eta \mathbf{P}_l}([\bar{\mathbf{z}}_{\kappa-1} - \eta \tilde{\nabla}_\kappa]_l) \\ &= \text{prox}_{\eta \mathbf{P}_l}([\mathbf{z}_{\kappa-1} - \eta \tilde{\nabla}_\kappa]_l) = [\mathbf{z}_\kappa]_l \end{aligned}$$

Thus we have $\bar{\mathbf{z}}_\kappa = \mathbf{z}_\kappa$. For $\bar{\mathbf{x}}_\kappa$, we have

$$\begin{aligned} \mathbf{x}_\kappa &= \bar{\mathbf{y}}_\kappa + \alpha_{2,s} B(\hat{\mathbf{z}}_j^s - \hat{\mathbf{z}}_{j-1}^s) \\ &= \beta_{j-1}^s \mathbf{u}_{j-1}^s + \gamma_s \hat{\mathbf{z}}_{j-1}^s + \alpha_{2,s} B(\hat{\mathbf{z}}_j^s - \hat{\mathbf{z}}_{j-1}^s) + \dot{\mathbf{x}}^s \\ &= \beta_{j-1}^s \mathbf{u}_j^s + \gamma_s \hat{\mathbf{z}}_j^s + \dot{\mathbf{x}}^s = \bar{\mathbf{x}}_\kappa \end{aligned}$$

due to the updating rule of \mathbf{u}_k in line 13 in AVRBCD II.

We then show that at the beginning of each epoch $\bar{\mathbf{z}}_k = \mathbf{z}_k$ and $\bar{\mathbf{x}}_k = \mathbf{x}_k$ stand. The idea here is that we are using iterates $\hat{\mathbf{z}}_j^s$ and \mathbf{u}_j^s from successive epochs to represent the same \mathbf{x}_k and \mathbf{z}_k . For \mathbf{z}_k , when $k = 0$,

$$\bar{\mathbf{z}}_0 = \hat{\mathbf{z}}_0^0 + \dot{\mathbf{x}}^0 = \mathbf{x}_0 = \mathbf{z}_0.$$

When $k = (s + 1)m$ with $s \geq 0$, we have

$$\mathbf{z}_{(s+1)m} \stackrel{a}{=} \bar{\mathbf{z}}_{sm+m} \stackrel{b}{=} \hat{\mathbf{z}}_0^{s+1} + \dot{\mathbf{x}}^{s+1} = \bar{\mathbf{z}}_{(s+1)m}$$

where the equation a is from the induction in previous epoch, and equation b is from the definition of $\hat{\mathbf{z}}_0^s$ in line 18 in AVRBCD II. For \mathbf{x}_k , we set $\beta_{-1}^s = 1$ (which is not used in practice). When $k = 0$, we clearly have $\mathbf{x}_0 = \bar{\mathbf{x}}_0$. When $k = (s + 1)m$ with $s \geq 0$, we have

$$\mathbf{x}_{(s+1)m} \stackrel{a}{=} \bar{\mathbf{x}}_{sm+m} \stackrel{b}{=} \beta_{-1}^s \mathbf{u}_0^{s+1} + \gamma_s \hat{\mathbf{z}}_0^s + \dot{\mathbf{x}}^s = \bar{\mathbf{x}}_{(s+1)m}.$$

where the equation a is from the induction in previous epoch, and equation b is from the definition of \mathbf{u}_0^s from line 19 in AVRBCD II. Thus we have the result. \square

Numerical Stability

Careful readers might have noticed that, since β_j^s decreases exponentially (line 14 in Algorithm 2), the computation of \mathbf{u}_j^s involving the inversion of β_j^s can be numerically unstable. To overcome this issue, we can simply keep their product $\beta_j^s \mathbf{u}_j^s = \xi \in \mathbb{R}^d$ in stead of themselves separately to make the computation numerically tractable. We also update ξ in a "lazy" manner so as to avoid high computation complexity. At the beginning of each epoch, we initialize a count vector $\omega \in \mathbb{R}^B$ to be a zero vector. In each of the following iterations, we do the follow steps

1. set $\omega_i = \omega_i + 1$ for all i ;
2. leave $[\xi]_{\setminus l}$ unchanged but update only $[\xi]_l$ as

$$[\xi]_l = \alpha_{1,s}^{\omega_l} [\xi]_l - (\alpha_{2,s} B + \gamma_s) (\hat{\mathbf{z}}_j^s - \hat{\mathbf{z}}_{j-1}^s) \quad (11)$$

where l is the block selected in that iteration;

3. set $\omega_l = 0$.

The idea is to use ω to record the exponential of $\alpha_{1,s}$ needs to be multiplied later. In this way, the exact computation of $\beta_j^s \mathbf{u}_j^s$ only happens at the end of each epoch.

Computational Complexity

Since the complexity of computing the partial gradient of some general convex function $f_i(\cdot)$ can be difficult to analyze, we mainly focus on the well-know Empirical Risk Minimization (ERM) problem with linear predictor, same as that in [5]. Under this setting, we can analyze the computational complexity of each inner loop as follows.

1. $\mathcal{O}(\Omega + B)$ from line 13, where $\mathcal{O}(B)$ is from the lazy update.
2. $\mathcal{O}(\rho d + B)$ from line 10, the computation of partial gradient, since (i) $\mathbf{a}_i^\top \dot{\mathbf{x}}^s$ can be kept when computing μ^s , (ii) $\mathbf{a}_i^\top \hat{\mathbf{z}}_j^s$ can be computed in $\mathcal{O}(\rho d)$, and (iii) $\mathbf{a}_i^\top \beta_j^s \mathbf{u}_j^s$ can be computed as $\sum_{l=1}^B \alpha_{1,s}^{\omega_l} [\mathbf{a}_i]_l^\top [\xi]_l$ in $\mathcal{O}(\rho d + B)$ where ξ is defined above. Recall that $\mathbf{a}_i^\top \bar{\mathbf{y}}_k = \mathbf{a}_i^\top (\beta_{j-1}^s \mathbf{u}_{j-1}^s + \gamma_s \hat{\mathbf{z}}_{j-1}^s + \dot{\mathbf{x}}^s)$.

Algorithm 2 AVRBCD II

Input: $m, \mathbf{x}_0, \alpha_{1,0}, \alpha_{2,0}$

- 1: $\mathbf{u}_0^0 = \hat{\mathbf{z}}_0^0 \leftarrow 0; \dot{\mathbf{x}}^0 \leftarrow \mathbf{x}_0;$
 - 2: **for** $s \leftarrow 0$ **to** S **do**
 - 3: $\alpha_{2,s} = \frac{\sqrt{\alpha_{2,s-1}^4 + 4\alpha_{2,s-1}^2 - \alpha_{2,s-1}^2}}{2};$
 - 4: $\alpha_{1,s} = \alpha_{1,s-1}(1 - \alpha_{2,s}), \alpha_{3,s} = 1 - \alpha_{1,s} - \alpha_{2,s};$
 - 5: $\bar{L}_s = \frac{L_Q}{B\alpha_{3,s}} + L_B, \eta_s = \frac{1}{L_s\alpha_{2,s}B};$
 - 6: $\mu^s = \nabla f(\dot{\mathbf{x}}^s);$
 - 7: **for** $j \leftarrow 1$ **to** m **do**
 - 8: $k = (sm) + j;$
 - 9: **sample** i **from** $\{1, \dots, n\}$ **and** l **from** $\{1, \dots, B\};$
 - 10: $\bar{\nabla}_k = \mu^s + \nabla f_i(\bar{\mathbf{y}}_k) - \nabla f_i(\bar{\mathbf{y}}_k);$
 - 11: $[\hat{\mathbf{z}}_j^s]_l = \text{prox}_{\eta \mathbf{P}_l}([\bar{\mathbf{z}}_k - \eta \bar{\nabla}_k]_l) - [\dot{\mathbf{x}}^s]_l;$
 - 12: $[\hat{\mathbf{z}}_j^s]_{\setminus l} = [\hat{\mathbf{z}}_{j-1}^s]_{\setminus l};$
 - 13: $\mathbf{u}_j^s = \mathbf{u}_{j-1}^s + \frac{\alpha_{2,s}B - \gamma_s}{\beta_{j-1}^s}(\hat{\mathbf{z}}_j^s - \hat{\mathbf{z}}_{j-1}^s);$
 - 14: $\beta_j^s = \alpha_{1,s}\beta_{j-1}^s;$
 - 15: **end for**
 - 16: **Sample** $\bar{\sigma}_s$ **from** $\{1, \dots, m\}$ **uniformly;**
 - 17: $\dot{\mathbf{x}}^{s+1} = \beta_{\bar{\sigma}_s-1}^s \mathbf{u}_{\bar{\sigma}_s}^s + \gamma_s \hat{\mathbf{z}}_{\bar{\sigma}_s}^s + \dot{\mathbf{x}}^s;$
 - 18: $\mathbf{x} = \bar{\mathbf{x}}_k - \dot{\mathbf{x}}^{s+1}, \hat{\mathbf{z}}_0^{s+1} = \bar{\mathbf{z}}_k - \dot{\mathbf{x}}^{s+1};$
 - 19: $\beta_0^{s+1} = \alpha_{1,s+1}, \mathbf{u}_0^{s+1} = \mathbf{x} - \gamma_{s+1} \hat{\mathbf{z}}_0^{s+1}$
 - 20: **end for**
-

3. $\mathcal{O}(\Omega)$ from the others.

Thus the overall computation complexity is $\mathcal{O}(\rho d + B + \Omega)$. When we pick a moderate B and the sparsity ρ is small, Ω will dominate the other two terms. This is the same per-iteration complexity as MRBCD and is much smaller than $\mathcal{O}(d)$ in methods like Katyusha and SVRG.

AVRBCD with Active Set

In MRBCD III, the authors use an active set strategy to further accelerate their method when solving sparse learning problems. We adapt such strategy to AVRBCD by modifying only two lines in AVRBCD II.

1. Add an operation

$$\dot{\mathbf{x}}^s = \text{prox}_{\frac{1}{L} \mathbf{P}}(\dot{\mathbf{x}}^s - \frac{1}{L} \mu^s) \quad (12)$$

below line 6.

2. In line 9, after we have selected block l , skip the rest operations in this iteration if $[\dot{\mathbf{x}}^s]_l = 0$.

In the first modification, the idea is to fully utilize the full gradient μ^s and produce a sparser snapshot $\dot{\mathbf{x}}^s$ with a proximal step. An empirical observation in our experiments

suggests that the support of the sparser snapshot provides a good prediction of the support of the optimal point \mathbf{x}^* , thus we omit the update on blocks out of the support of $\tilde{\mathbf{x}}^s$ in the second modification. Such active set strategy is common in the RBCD literature, and usually boosts the empirical performance [6, 24].

Convergence Analysis

We give the convergence results of AVRBCD under both non-proximal ($\mathbf{P}(\mathbf{x}) \equiv 0$) and proximal ($\mathbf{P}(\mathbf{x}) \neq 0$) settings. In the former case, we show that AVRBCD takes $\mathcal{O}((n + \sqrt{nL})/\sqrt{\epsilon})$ iterations to obtain an ϵ -accurate solution, while in the latter case, $\mathcal{O}(\sqrt{B}(n + \sqrt{nL})/\sqrt{\epsilon})$ iterations are needed to achieve the same accuracy. We believe the additional \sqrt{B} factor is the artifact of our proof as we do not observe such phenomenon in experiments.

Non-Proximal Case ($\mathbf{P}(\mathbf{x}) \equiv 0$)

First, let us establish an inequality that relates the objective values between two successive iterations. Define

$$d(\mathbf{x}) = \mathbf{F}(\mathbf{x}) - \mathbf{F}(\mathbf{x}^*)$$

to be the sub-optimality at \mathbf{x} , we have the following lemma.

Lemma 1. *In Algorithm 1, we have*

$$\begin{aligned} \mathbb{E}_{l,i_k} d(\mathbf{x}_k) &\leq \alpha_{3,s} d(\tilde{\mathbf{x}}^s) + \alpha_{1,s} d(\mathbf{x}_{k-1}) \\ &\quad + \frac{\bar{L}_s \alpha_{2,s}^2 B^2}{2} (\|\mathbf{x}^* - \mathbf{z}_{k-1}\|^2 - \mathbb{E}_{l,i_k} \|\mathbf{x}^* - \mathbf{z}_k\|^2) \end{aligned}$$

The proof of this lemma in the appendix. We will prove Theorem 1 based on Lemma 1.

Theorem 1 (Non-Proximal). *By setting $\alpha_{2,0} = \frac{2}{\nu}$, $0 < \alpha_{3,0} \leq \frac{\nu-2}{\nu}$, and $\alpha_{1,0} = 1 - \alpha_{2,0} - \alpha_{3,0}$, with $\nu > 2$, we have*

$$d(\tilde{\mathbf{x}}^s) \leq \frac{\alpha_{2,s}^2}{\alpha_{3,s}} \left(\frac{\alpha_{1,0}}{\alpha_{2,0}^2} \frac{d(\mathbf{x}_0)}{m} + \frac{\alpha_{3,0}}{\alpha_{2,0}^2} d(\mathbf{x}_0) + \frac{\bar{L}_0 B^2}{2m} \|\mathbf{x}^* - \mathbf{x}_0\|^2 \right)$$

Proof. The expectations are taken with respect to all history randomness, and are omitted for simplicity. Use d_k to denote $d(\mathbf{x}_k)$ and \tilde{d}_s to denote $d(\tilde{\mathbf{x}}^s)$. Dividing both sides of Lemma 1 by $\alpha_{2,s}^2$ and summing from $k = sm + 1$ to $(s + 1)m$, we get

$$\begin{aligned} \frac{1}{\alpha_{2,s}^2} \sum_{j=1}^m d_{sm+j} &\leq \frac{\alpha_{1,s}}{\alpha_{2,s}^2} \sum_{j=0}^{m-1} d_{sm+j} + \frac{\alpha_{3,s}}{\alpha_{2,s}^2} m \tilde{d}^s \\ &\quad + \frac{\bar{L}_s B^2}{2} \{ \|\mathbf{x}^* - \mathbf{z}_{sm}\|^2 - \|\mathbf{x}^* - \mathbf{z}_{sm+m}\|^2 \}. \end{aligned}$$

By rearranging terms, we have

$$\begin{aligned} \frac{\alpha_{1,s}}{\alpha_{2,s}^2} d_{sm+m} + \frac{1-\alpha_{1,s}}{\alpha_{2,s}^2} \sum_{j=1}^m d_{sm+j} &\leq \frac{\alpha_{1,s}}{\alpha_{2,s}^2} d_{sm} + \frac{\alpha_{3,s}}{\alpha_{2,s}^2} m \tilde{d}_s \\ &+ \frac{\bar{L}_s B^2}{2} \{ \|\mathbf{x}^* - \mathbf{z}_{0,s}\|^2 - \|\mathbf{x}^* - \mathbf{z}_{m,s}\|^2 \}. \end{aligned}$$

Using the fact that $\frac{1-\alpha_{1,s}}{\alpha_{2,s}^2} = \frac{\alpha_{3,s+1}}{\alpha_{2,s+1}^2}$, $\frac{1}{\alpha_{2,s}^2} = \frac{1-\alpha_{2,s+1}}{\alpha_{2,s+1}^2}$, we have $\frac{\alpha_{1,s}}{\alpha_{2,s}^2} = \frac{\alpha_{1,s+1}}{\alpha_{2,s+1}^2}$. From the definition of $\tilde{\mathbf{x}}^s$, we have $m \tilde{d}_{s+1} \leq \sum_{j=1}^m d_{sm+j}$. Additionally, using $\bar{L}_{s+1} \leq \bar{L}_s$, we have the following inequality

$$\begin{aligned} \frac{\alpha_{1,s+1}}{\alpha_{2,s+1}^2} d_{sm+m} + \frac{\alpha_{3,s+1}}{\alpha_{2,s+1}^2} m \tilde{d}_{s+1} + \frac{\bar{L}_{s+1} B^2}{2} \|\mathbf{x}^* - \mathbf{z}_{sm+m}\|^2 \\ \leq \frac{\alpha_{1,s}}{\alpha_{2,s}^2} d_{sm} + \frac{\alpha_{3,s}}{\alpha_{2,s}^2} m \tilde{d}_s + \frac{\bar{L}_s B^2}{2} \|\mathbf{x}^* - \mathbf{z}_{sm}\|^2. \end{aligned}$$

By the non-negativity of $d(\cdot)$, we have the result. \square

The following relations come from the constructions of $\{\alpha_{i,s}\}_{i=1}^3$,

1. $\alpha_{2,s} \leq \alpha_{2,s-1}$, $\alpha_{1,s} \leq \alpha_{1,s-1}$, and thus $\alpha_{3,s} \geq \alpha_{3,s-1}$;
2. $\alpha_{2,s} \leq 2/(s+\nu)$, if $\alpha_{2,s-1} \leq 2/(s+\nu-1)$.

From such relations, we have the corollary to describe the convergence rate of AVRBCD in non-proximal case.

Corollary 1. *By setting $m = Bn$, we have*

$$d(\tilde{\mathbf{x}}^s) \leq \frac{Cd(\mathbf{x}_0) + \frac{\bar{L}}{n} \|\mathbf{x}^* - \mathbf{x}_0\|^2}{s^2}$$

where C is some constant.

In other words, to obtain an ϵ -accurate solution, AVRBCD need $\sqrt{(Cd(\mathbf{x}_0) + \frac{\bar{L}}{n} \|\mathbf{x}^ - \mathbf{x}_0\|^2)/\epsilon}$ iterations.*

Proximal Case ($\mathbf{P}(\mathbf{x}) \neq 0$)

The key idea to prove the convergence of proximal version of AVRBCD is to express \mathbf{x}_k as the convex combination of $\{\tilde{\mathbf{x}}^i\}_{i=0}^s$ and $\{\mathbf{z}_l\}_{l=0}^k$.

Lemma 2. *In Algorithm 1, by setting $\alpha_{2,0} = \alpha_{3,0} = 1/2B$, for $k = sm + j \geq 1$, we have*

$$\mathbf{x}_k = \sum_{i=0}^{s-1} \lambda_k^i \tilde{\mathbf{x}}^i + \beta_j^s \tilde{\mathbf{x}}^s + \sum_{l=0}^k \gamma_k^l \mathbf{z}_l \quad (13)$$

where $\gamma_0^0 = 1$, $\gamma_1^0 = \frac{1}{2} - \frac{1}{2B}$, $\gamma_1^1 = \frac{1}{2}$, $\beta_0^0 = 0$, $\lambda_{(s+1)m}^s = \beta_m^s$, $\lambda_{k+1}^i = \alpha_{1,s}\lambda_k^i$

$$\gamma_{k+1}^l = \begin{cases} \alpha_{1,s}\gamma_k^l, & l = 0, \dots, k-1 \\ B\alpha_{1,s}\alpha_{2,s} + (1-B)\alpha_{2,s}, & l = k \\ B\alpha_{2,s}, & l = k+1 \end{cases}$$

and

$$\beta_{j+1}^s = \alpha_{1,s}\beta_j^s + \alpha_{3,s}. \quad (14)$$

Additionally, we have $\sum_{i=0}^{s-1} \lambda_k^i + \beta_j^s + \sum_{l=0}^k \gamma_k^l = 1$ and each entry in this sum is non-negative for all $k \geq 1$, i.e. \mathbf{x}_k is a convex combination of $\{\tilde{\mathbf{x}}^i\}_{i=0}^s$ and $\{\mathbf{z}_l\}_{l=0}^k$.

From Lemma 5 and the convexity of $\mathbf{P}(\cdot)$, we have

$$\mathbf{P}(\mathbf{x}_k) \leq \sum_{i=0}^{s-1} \lambda_k^i \mathbf{P}(\tilde{\mathbf{x}}^i) + \beta_j^s \mathbf{P}(\tilde{\mathbf{x}}^s) + \sum_{l=0}^k \gamma_k^l \mathbf{P}(\mathbf{z}_l) \stackrel{\text{def}}{=} \hat{\mathbf{P}}(\mathbf{x}_k).$$

We also define the sub-optimality $d(\mathbf{x})$ and its upper bound $\hat{d}(\mathbf{x}_k)$ at \mathbf{x}_k as

$$\begin{aligned} d(\mathbf{x}_k) &= (\mathbf{F}(\mathbf{x}_k) + \mathbf{P}(\mathbf{x}_k)) - (\mathbf{F}(\mathbf{x}^*) + \mathbf{P}(\mathbf{x}^*)), \\ \hat{d}_k &= (\mathbf{F}(\mathbf{x}_k) + \hat{\mathbf{P}}(\mathbf{x}_k)) - (\mathbf{F}(\mathbf{x}^*) + \mathbf{P}(\mathbf{x}^*)). \end{aligned}$$

For \hat{d}_k , we have $0 \leq d(\mathbf{x}_k) \leq \hat{d}_k$ and $d(\mathbf{x}_0) = \hat{d}_0$.

Lemma 3. In Algorithm 1, by setting $\alpha_{2,0} = \alpha_{3,0} = 1/2B$,

$$\begin{aligned} \mathbb{E}_{l,i_k} \hat{d}_k &\leq \alpha_{3,s} d(\tilde{\mathbf{x}}^s) + \alpha_{1,s} \hat{d}_{k-1} \\ &\quad + \frac{\bar{L}_s \alpha_{2,s}^2 B^2}{2} (\|\mathbf{x}^* - \mathbf{z}_{k-1}\|^2 - \mathbb{E}_{l,i_k} \|\mathbf{x}^* - \mathbf{z}_k\|^2) \end{aligned}$$

This lemma is similar to Lemma 1, but harder to prove due to the regularization term \mathbf{P} . Again, we use it to prove Theorem 3. The proof is similar to that of Theorem 1.

Theorem 2. By setting $\alpha_{2,0} = \alpha_{3,0} = \frac{1}{2B}$ and $\alpha_{1,0} = 1 - \alpha_{2,0} - \alpha_{3,0}$, we have

$$d(\tilde{\mathbf{x}}^s) \leq \frac{\alpha_{2,s}^2}{\alpha_{3,s}} \left(\frac{\alpha_{1,0}}{\alpha_{2,0}} \frac{d(\mathbf{x}_0)}{m} + \frac{\alpha_{3,0}}{\alpha_{2,0}} d(\mathbf{x}_0) + \frac{\bar{L}_0 B^2}{2m} \|\mathbf{x}^* - \mathbf{x}_0\|^2 \right)$$

Again, we have the corollary to describe the convergence rate of AVRBCD in proximal case.

Corollary 2. By setting $m = Bn$, we have

$$d(\tilde{\mathbf{x}}^s) \leq \frac{B(Cd(\mathbf{x}_0) + \frac{\bar{L}}{n} \|\mathbf{x}^* - \mathbf{x}_0\|^2)}{s^2}$$

where C is some constant.

In other words, to obtain an ϵ -accurate solution, AVRBCD need $\sqrt{B(Cd(\mathbf{x}_0) + \frac{\bar{L}}{n} \|\mathbf{x}^* - \mathbf{x}_0\|^2)/\epsilon}$ iterations.

Table 1: Statistics of datasets.

Dataset	n	d	sparsity
real-sim	72,309	20,958	0.24%
rcv1	20,242	47,236	0.16%
news20.binary	19,996	1,355,191	0.0336%

Overall Complexity

Combining with the analysis of per-iteration complexity in the previous section and the convergence rate discussed above, the overall computational complexity of AVRBCD in the sparse ERM problems is $\mathcal{O}(nd/\sqrt{\epsilon} + d\sqrt{\bar{L}n}/\sqrt{\epsilon})$ for non-proximal case, and $\mathcal{O}(nd\sqrt{B}/\sqrt{\epsilon} + d\sqrt{\bar{L}nB}/\sqrt{\epsilon})$ for proximal case. This is similar to Katyusha, i.e. $\mathcal{O}(nd/\sqrt{\epsilon} + d\sqrt{L_{max}n}/\sqrt{\epsilon})$ in both proximal or non-proximal case, and is better than $\mathcal{O}(ndBL_B/\sqrt{\epsilon})$ in APPROX and $\mathcal{O}((nd + dL_{max}/\epsilon) \log \frac{1}{\epsilon})$ in MRBCD II.

Experiments

In this section, we present results of several numerical experiments to validate our analysis for AVRBCD and to show the effectiveness of AVRBCD with active set (AVRBCD-AC) on real problems. Empirical studies on l_1 -logistic regression and l_1l_2 -logistic regression are conducted. Three large scale datasets from LibSVM are used, namely real-sim, rcv1, and news20.binary, all of which have large number of samples and features ($n, d > 10^4$). The statistics are given in Table 1 along with the sparsity of the datasets. Katyusha with opt.II [1], MRBCD II and III [27], and SVRG [9] are included in comparison. We use the parameter suggested in the original paper for Katyusha. For SVRG, we set the inner loop count $m = n$ and the step size $\eta = 1/2L_{max}$. We also incorporate the mini-batch technique in our methods and set the mini batch size to 8, same as that of MRBCD II and III. The step sizes for MRBCD II and III are set to $4/L_{max}$ which gives the best performance in our experiments. For AVRBCD and AVRBCD-AC, the step sizes are set to $4/L_{max}\alpha_{2,s}$ which increases as iteration goes on, similar to Katyusha. For MRBCD II and III, AVRBCD, and AVRBCD-AC, we set $m = nB/8$. As for initialization, \mathbf{x}_0 is set to zero in all experiments. We define the *log-suboptimality* at \mathbf{x} as $\log_{10}(\mathbf{F}^{\mathbf{P}}(\mathbf{x}) - \mathbf{F}^{\mathbf{P}}(\mathbf{x}^*))$ and the *effective pass* as the evaluation of nd component partial gradients. These quantities are used to evaluate the performance of the algorithms [27]. Due to the randomness of the algorithms, the reported results are the average of 10 independent trials.

l_1 -Logistic Regression

Three datasets are used in l_1 -Logistic Regression, namely rcv1, real-sim, and news20.binary. Here, the component function is $f_i(\mathbf{x}) = \log(1 + \exp(-y_i\mathbf{a}_i^\top \mathbf{x}))$ and the regularization function is $\mathbf{P}(\mathbf{x}) = \lambda_1\|\mathbf{x}\|_1$, where (\mathbf{a}_i, y_i) correspond to the feature vector and response of the i^{th} sample respectively. In all experiments, λ_1 is set to 10^{-5} . We compare the convergence rate in Figure 1. The result shows that (i) Katyusha and AVRBCD

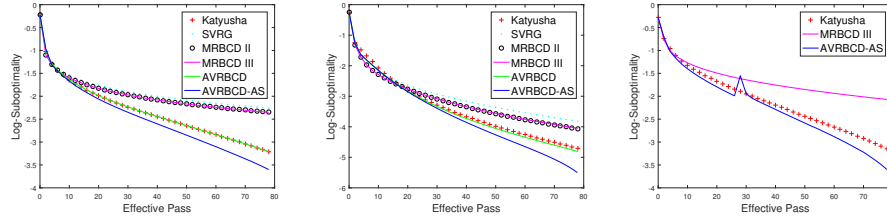


Figure 1: l_1 -Logistic Regression. From left to right are results on rcv1, real_sim, and news20.binary

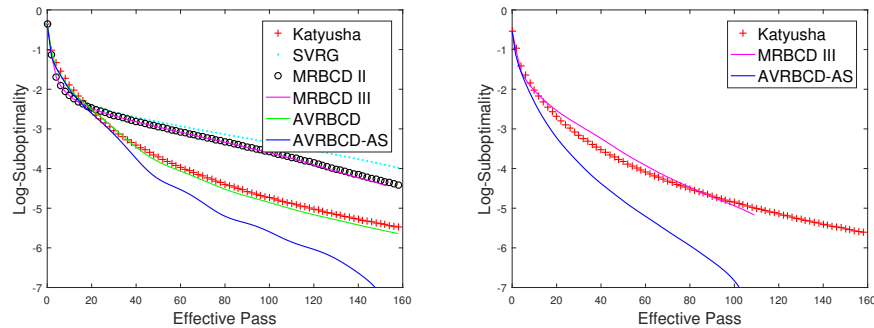


Figure 2: l_1l_2 -Logistic Regression. From left to right are results on rcv1 and news20.binary

have the similar amount of overall partial gradient evaluations, conforming to our analysis, and (ii) AVRBCD-AS has the best performance among all competitors. Since MRBCD III has the best performance among all non-accelerated methods, we only include MRBCD III, Katyusha, and AVRBCD III in our experiment on news20.binary.

l_1l_2 -Logistic Regression

Rcv1 and news20.binary are used to test the performance of our methods in l_1l_2 -Logistic Regression. We set $f_i(\mathbf{x}) = \log(1 + \exp(-y_i \mathbf{a}_i^\top \mathbf{x})) + \frac{\lambda_2}{2} \|\mathbf{x}\|^2$ and $\mathbf{P}(\mathbf{x}) = \lambda_1 \|\mathbf{x}\|_1$, as suggested in [25]. In all experiments, λ_1 is set to 10^{-4} and λ_2 is set to 10^{-8} . The results shows the similar phenomenon as in l_1 -Logistic Regression, and our methods have the best computational efficiency.

Conclusion

In this paper, we proposed an accelerated variance reduced block coordinate descent algorithm that can handle problems with large number of samples in ultra-high dimensional space. We compare our algorithms to state of the arts in large scale sparse learning problems, and the result is outstanding.

References

- [1] Zeyuan Allen-Zhu. Katyusha: Accelerated variance reduction for faster sgd. *arXiv preprint arXiv:1603.05953*, 2016.
- [2] Zeyuan Allen-Zhu and Yang Yuan. Even faster accelerated coordinate descent using non-uniform sampling. *arXiv preprint arXiv:1512.09103*, 2015.
- [3] Zeyuan Allen-Zhu and Yang Yuan. Improved svrg for non-strongly-convex or sum-of-non-convex objectives. *arXiv preprint arXiv:1506.01972*, 2015.
- [4] Aaron Defazio, Francis Bach, and Simon Lacoste-Julien. Saga: A fast incremental gradient method with support for non-strongly convex composite objectives. In *Advances in Neural Information Processing Systems*, pages 1646–1654, 2014.
- [5] Olivier Fercoq and Peter Richtárik. Accelerated, parallel, and proximal coordinate descent. *SIAM Journal on Optimization*, 25(4):1997–2023, 2015.
- [6] Jerome Friedman, Trevor Hastie, Holger Höfling, Robert Tibshirani, et al. Pathwise coordinate optimization. *The Annals of Applied Statistics*, 1(2):302–332, 2007.
- [7] Roy Frostig, Rong Ge, Sham M Kakade, and Aaron Sidford. Un-regularizing: approximate proximal point and faster stochastic algorithms for empirical risk minimization. In *Proceedings of the 32nd International Conference on Machine Learning (ICML)*, 2015.
- [8] Le Thi Khanh Hien, Canyi Lu, Huan Xu, and Jiashi Feng. Accelerated stochastic mirror descent algorithms for composite non-strongly convex optimization. *arXiv preprint arXiv:1605.06892*, 2016.
- [9] Rie Johnson and Tong Zhang. Accelerating stochastic gradient descent using predictive variance reduction. In *Advances in Neural Information Processing Systems*, pages 315–323, 2013.
- [10] Jakub Konecny, Zheng Qu, and Peter Richtárik. S2cd: Semi-stochastic coordinate descent. In *NIPS Optimization in Machine Learning workshop*, 2014.
- [11] Jakub Konecny and Peter Richtárik. Semi-stochastic gradient descent methods. 2013.
- [12] Yin Tat Lee and Aaron Sidford. Efficient accelerated coordinate descent methods and faster algorithms for solving linear systems. In *Foundations of Computer Science (FOCS), 2013 IEEE 54th Annual Symposium on*, pages 147–156. IEEE, 2013.
- [13] Hongzhou Lin, Julien Mairal, and Zaid Harchaoui. A universal catalyst for first-order optimization. In *Advances in Neural Information Processing Systems*, pages 3384–3392, 2015.
- [14] Ji Liu and Stephen J Wright. Asynchronous stochastic coordinate descent: Parallelism and convergence properties. *SIAM Journal on Optimization*, 25(1):351–376, 2015.
- [15] Mehrdad Mahdavi, Lijun Zhang, and Rong Jin. Mixed optimization for smooth functions. In *Advances in Neural Information Processing Systems*, pages 674–682, 2013.
- [16] Yu Nesterov. Efficiency of coordinate descent methods on huge-scale optimization problems. *SIAM Journal on Optimization*, 22(2):341–362, 2012.
- [17] Zheng Qu and Peter Richtárik. Coordinate descent with arbitrary sampling i: Algorithms and complexity. *arXiv preprint arXiv:1412.8060*, 2014.
- [18] Zheng Qu and Peter Richtárik. Coordinate descent with arbitrary sampling ii: Expected separable overapproximation. *arXiv preprint arXiv:1412.8063*, 2014.

- [19] Sashank J Reddi, Ahmed Hefny, Suvrit Sra, Barnabas Poczos, and Alex J Smola. On variance reduction in stochastic gradient descent and its asynchronous variants. In *Advances in Neural Information Processing Systems*, pages 2647–2655, 2015.
- [20] Peter Richtárik and Martin Takáč. Iteration complexity of randomized block-coordinate descent methods for minimizing a composite function. *Mathematical Programming*, 144(1-2):1–38, 2014.
- [21] Peter Richtárik and Martin Takáč. Parallel coordinate descent methods for big data optimization. *Mathematical Programming*, 156(1-2):433–484, 2016.
- [22] Mark Schmidt, Nicolas Le Roux, and Francis Bach. Minimizing finite sums with the stochastic average gradient. *arXiv preprint arXiv:1309.2388*, 2013.
- [23] Stephen J Wright. Coordinate descent algorithms. *Mathematical Programming*, 151(1):3–34, 2015.
- [24] Tong Tong Wu and Kenneth Lange. Coordinate descent algorithms for lasso penalized regression. *The Annals of Applied Statistics*, pages 224–244, 2008.
- [25] Lin Xiao and Tong Zhang. A proximal stochastic gradient method with progressive variance reduction. *SIAM Journal on Optimization*, 24(4):2057–2075, 2014.
- [26] Yuchen Zhang and Lin Xiao. Stochastic primal-dual coordinate method for regularized empirical risk minimization. In *Proceedings of the 32nd International Conference on Machine Learning*, volume 951, page 2015, 2015.
- [27] Tuo Zhao, Mo Yu, Yiming Wang, Raman Arora, and Han Liu. Accelerated mini-batch randomized block coordinate descent method. In *Advances in neural information processing systems*, pages 3329–3337, 2014.

Appendix

This appendix gives the proof for Lemma 1 and Theorem 2 in the AAAI paper.

Proof of Lemma 1

Lemma 4.

$$\mathbb{E}_k[\|\mathbf{z}_k - \mathbf{x}\|^2] = \frac{1}{m} \|\tilde{\mathbf{z}}_k - \mathbf{x}\|^2 + \frac{m-1}{m} \|\mathbf{z}_{k-1} - \mathbf{x}\|^2 \quad (15)$$

$$\mathbb{E}_k[\mathbf{P}(\mathbf{z}_k)] = \frac{1}{m} \mathbf{P}(\tilde{\mathbf{z}}_k) + \frac{m-1}{m} \mathbf{P}(\mathbf{z}_{k-1}) \quad (16)$$

Lemma 5. In Algorithm 1, by setting $\alpha_{2,0} = \alpha_{3,0} = 1/2B$, for $k = sm + j \geq 1$, we have

$$\mathbf{x}_k = \sum_{i=0}^{s-1} \lambda_k^i \tilde{\mathbf{x}}^i + \beta_j^s \tilde{\mathbf{x}}^s + \sum_{l=0}^k \gamma_k^l \mathbf{z}_l \quad (17)$$

where $\gamma_0^0 = 1$, $\gamma_1^0 = \frac{1}{2} - \frac{1}{2B}$, $\gamma_1^1 = \frac{1}{2}$, $\beta_0^0 = 0$, $\lambda_{(s+1)m}^s = \beta_m^s$, $\lambda_{k+1}^i = \alpha_{1,s} \lambda_k^i$

$$\gamma_{k+1}^l = \begin{cases} \alpha_{1,s} \gamma_k^l, & l = 0, \dots, k-1 \\ B\alpha_{1,s} \alpha_{2,s} + (1-B)\alpha_{2,s}, & l = k \\ B\alpha_{2,s}, & l = k+1 \end{cases}$$

and

$$\beta_{j+1}^s = \alpha_{1,s}\beta_j^s + \alpha_{3,s}. \quad (18)$$

Additionally, we have $\sum_{i=0}^{s-1} \lambda_k^i + \beta_j^s + \sum_{l=0}^k \gamma_k^l = 1$ and each entry in this sum is non-negative for all $k \geq 1$, i.e. \mathbf{x}_k is a convex combination of $\{\tilde{\mathbf{x}}^i\}_{i=0}^s$ and $\{\mathbf{z}_l\}_{l=0}^k$.

Proof. When $s = 0$,

$$\begin{aligned} \mathbf{x}_0 &= \mathbf{z}_0 \\ \mathbf{y}_1 &= \alpha_{1,0}\mathbf{z}_0 + \alpha_{2,0}\mathbf{z}_0 + \alpha_{3,0}\tilde{\mathbf{x}} \\ \mathbf{x}_1 &= (\alpha_{1,0} + \alpha_{2,0})\mathbf{z}_0 + B\alpha_{2,0}(\mathbf{z}_1 - \mathbf{z}_0) + \alpha_{3,0}\tilde{\mathbf{x}}^0 \\ &= \left(\frac{1}{2} - \alpha_{3,0}\right)\mathbf{z}_0 + \frac{1}{2}\mathbf{z}_1 + \alpha_{3,0}\tilde{\mathbf{x}}^0 \end{aligned}$$

which proves the initialization. We prove by induction. Assume that our formulation is correct up till the κ^{th} iteration. In the following iterations,

$$\begin{aligned} \mathbf{y}_{\kappa+1} &= \alpha_{1,0}\mathbf{x}_\kappa + \alpha_{2,0}\mathbf{z}_\kappa + \alpha_{3,0}\tilde{\mathbf{x}} \\ \mathbf{x}_{\kappa+1} &= \alpha_{1,0}\mathbf{x}_\kappa + \alpha_{2,0}\mathbf{z}_\kappa + \alpha_{3,0}\tilde{\mathbf{x}} + \alpha_{2,0}B(\mathbf{z}_{\kappa+1} - \mathbf{z}_\kappa) \\ &= \alpha_{1,0} \sum_{l=1}^{\kappa-1} \gamma_\kappa^l \mathbf{z}_l + (B\alpha_{1,s}\alpha_{2,s} + (1-B)\alpha_{2,s})\mathbf{z}_\kappa \\ &\quad + B\alpha_{2,s}\mathbf{z}_{\kappa+1} + (\alpha_{1,0}\beta_j^0 + \alpha_{3,0})\tilde{\mathbf{x}} \end{aligned}$$

which gives us the result. When $s \geq 1$, the same induction holds except the additional $\sum_{i=0}^{s-1} \lambda_k^i \tilde{\mathbf{x}}^i$. See that $\tilde{\mathbf{x}}^i$ is only added after the i^{th} epoch is done. So it should be initialized as $\lambda_{k+1}^i = \alpha_{1,s}\lambda_k^i$. \square

Proof of Theorem 2

Suppose in the k^{th} iteration, function i_k is sampled from all n subfunctions and block l_k is sampled from all B blocks. Define $\tilde{\mathbf{z}}_k$ to be the vector if all B blocks are updated in the k^{th} iteration, i.e. $\tilde{\mathbf{z}}_k = \text{prox}_{\eta_s \mathbf{P}_l}(\mathbf{z}_{k-1} - \alpha_s \mathbf{v}_k)$. Clearly, for all $l \in [B]$ we have

$$[\mathbf{z}_k]_l = \begin{cases} [\tilde{\mathbf{z}}_k]_l & l = l_k, \\ [\mathbf{z}_{k-1}]_l & l \neq l_k. \end{cases} \quad (19)$$

Theorem 3. By setting $\alpha_{2,0} = \alpha_{3,0} = \frac{1}{2B}$ and $\alpha_{1,0} = 1 - \alpha_{2,0} - \alpha_{3,0}$, we have

$$d(\tilde{\mathbf{x}}^s) \leq \frac{\alpha_{2,s}^2}{\alpha_{3,s}} \left(\frac{\alpha_{1,0}}{\alpha_{2,0}^2} \frac{d(\mathbf{x}_0)}{m} + \frac{\alpha_{3,0}}{\alpha_{2,0}^2} d(\mathbf{x}_0) + \frac{\bar{L}_0 B^2}{2m} \|\mathbf{x}^* - \mathbf{x}_0\|^2 \right)$$

Proof. From Lemma 5, we have

$$\mathbf{P}(\mathbf{x}_k) \leq \sum_{i=0}^{s-1} \lambda_k^i \mathbf{P}(\tilde{\mathbf{x}}^i) + \beta_k \mathbf{P}(\tilde{\mathbf{x}}) + \sum_{l=0}^k \gamma_k^l \mathbf{P}(\mathbf{z}_l) \stackrel{\text{def}}{=} \hat{\mathbf{P}}(\mathbf{x}_k). \quad (20)$$

Using (16) in Lemma 4, we have

$$\begin{aligned}
\mathbb{E}_k \hat{\mathbf{P}}(\mathbf{x}_k) &= \sum_{i=0}^{s-1} \lambda_k^i \mathbf{P}(\tilde{\mathbf{x}}^i) + \beta_k \mathbf{P}(\tilde{\mathbf{x}}) + \sum_{l=0}^{k-1} \gamma_k^l \mathbf{P}(\mathbf{z}_l) + m\alpha_2 \mathbb{E}_k \mathbf{P}(\mathbf{z}_k) \\
&= \sum_{i=0}^{s-1} \lambda_k^i \mathbf{P}(\tilde{\mathbf{x}}^i) + \beta_k \mathbf{P}(\tilde{\mathbf{x}}) + \sum_{l=0}^{k-1} \gamma_k^l \mathbf{P}(\mathbf{z}_l) \\
&\quad + \alpha_2(m-1) \mathbf{P}(\mathbf{z}_{k-1}) + \alpha_2 \mathbf{P}(\tilde{\mathbf{z}}_k).
\end{aligned}$$

Assume that in the k^{th} iteration, the l^{th} block is selected. Let L_l be the Lipschitz smoothness parameter of function \mathbf{F} in the l^{th} block and define $L_B = \max_l L_l$

$$\begin{aligned}
&\mathbf{F}(\mathbf{x}_k) \\
&\leq \mathbf{F}(\mathbf{y}_k) + \langle [\nabla \mathbf{F}(\mathbf{y}_k)]_l, [\mathbf{x}_k - \mathbf{y}_k]_l \rangle + \frac{L_l}{2} \|\mathbf{x}_k - \mathbf{y}_k\|_l^2 \\
&= \mathbf{F}(\mathbf{y}_k) + \langle [\nabla \mathbf{F}(\mathbf{y}_k) - \mathbf{v}_k]_l, [\mathbf{x}_k - \mathbf{y}_k]_l \rangle + \frac{L_l}{2} \|\mathbf{x}_k - \mathbf{y}_k\|_l^2 \\
&\quad + \langle [\mathbf{v}_k]_l, [\mathbf{x}_k - \mathbf{y}_k]_l \rangle \\
&\leq \mathbf{F}(\mathbf{y}_k) + \frac{L_Q}{2B\alpha_{3,s}} \|\mathbf{x}_k - \mathbf{y}_k\|_l^2 + \frac{B\alpha_{3,s}}{2L_Q} \|[\nabla \mathbf{F}(\mathbf{y}_k) - \mathbf{v}_k]_l\|^2 \\
&\quad + \frac{L_l}{2} \|\mathbf{x}_k - \mathbf{y}_k\|_l^2 + \langle [\mathbf{v}_k]_l, [\mathbf{x}_k - \mathbf{y}_k]_l \rangle \\
&= \mathbf{F}(\mathbf{y}_k) + \frac{\bar{L}_s}{2} \|\mathbf{x}_k - \mathbf{y}_k\|_l^2 + \frac{B\alpha_{3,s}}{2L_Q} \|[\nabla \mathbf{F}(\mathbf{y}_k) - \mathbf{v}_k]_l\|^2 \\
&\quad + \langle [\mathbf{v}_k]_l, [\mathbf{x}_k - \mathbf{y}_k]_l \rangle \\
&= \mathbf{F}(\mathbf{y}_k) + \frac{B\alpha_{3,s}}{2L_Q} \|[\nabla \mathbf{F}(\mathbf{y}_k) - \mathbf{v}_k]_l\|^2 + B\alpha_{2,s} \langle [\mathbf{v}_k]_l, [\tilde{\mathbf{z}}_k - \mathbf{z}_{k-1}]_l \rangle \\
&\quad + \frac{\bar{L}_s \alpha_{2,s}^2 B^2}{2} \|[\tilde{\mathbf{z}}_k - \mathbf{z}_{k-1}]_l\|^2
\end{aligned}$$

Taking expectation with respect to l , we have

$$\begin{aligned}
&\mathbb{E}_l \mathbf{F}(\mathbf{x}_k) \\
&\leq \mathbf{F}(\mathbf{y}_k) + \frac{B\alpha_{3,s}}{2L_Q} \mathbb{E}_l \|[\nabla \mathbf{F}(\mathbf{y}_k) - \mathbf{v}_k]_l\|^2 + B\alpha_{2,s} \mathbb{E}_l \langle [\mathbf{v}_k]_l, [\tilde{\mathbf{z}}_k - \mathbf{z}_{k-1}]_l \rangle \\
&\quad + \frac{\bar{L}_s \alpha_{2,s}^2 B^2}{2} \mathbb{E}_l \|[\tilde{\mathbf{z}}_k - \mathbf{z}_{k-1}]_l\|^2 \\
&= \mathbf{F}(\mathbf{y}_k) + \frac{\alpha_{3,s}}{2L_Q} \|\nabla \mathbf{F}(\mathbf{y}_k) - \mathbf{v}_k\|^2 + \alpha_{2,s} \langle \mathbf{v}_k, \tilde{\mathbf{z}}_k - \mathbf{z}_{k-1} \rangle \\
&\quad + \frac{\bar{L}_s \alpha_{2,s}^2 B}{2} \|\tilde{\mathbf{z}}_k - \mathbf{z}_{k-1}\|^2.
\end{aligned}$$

Add the regularization term and use (20).

$$\begin{aligned}
& \mathbb{E}_l \mathbf{F}(\mathbf{x}_k) + \hat{\mathbf{P}}(\mathbf{x}_k) \\
\leq & \mathbf{F}(\mathbf{y}_k) + \frac{\alpha_{3,s}}{2L_Q} \|\nabla \mathbf{F}(\mathbf{y}_k) - \mathbf{v}_k\|^2 + \alpha_{2,s} \langle \mathbf{v}_k, \tilde{\mathbf{z}}_k - \mathbf{z}_{k-1} \rangle + \frac{\bar{L}_s \alpha_{2,s}^2 B}{2} \|\tilde{\mathbf{z}}_k - \mathbf{z}_{k-1}\|^2 + \mathbb{E}_l \hat{\mathbf{P}}(\mathbf{x}_k) \\
= & \mathbf{F}(\mathbf{y}_k) + \alpha_{3,s} \left\{ \frac{1}{2L_Q} \|\nabla \mathbf{F}(\mathbf{y}_k) - \mathbf{v}_k\|^2 + \langle \nabla \mathbf{F}(\mathbf{y}_k), \tilde{\mathbf{x}} - \mathbf{y}_k \rangle \right\} \\
& + \alpha_{2,s} \langle \mathbf{v}_k, \tilde{\mathbf{z}}_k - \mathbf{z}_{k-1} \rangle + \frac{\bar{L}_s \alpha_{2,s}^2 B}{2} \|\tilde{\mathbf{z}}_k - \mathbf{z}_{k-1}\|^2 - \alpha_{3,s} \langle \nabla \mathbf{F}(\mathbf{y}_k), \tilde{\mathbf{x}} - \mathbf{y}_k \rangle \\
& + \sum_{i=0}^{s-1} \lambda_k^i \mathbf{P}(\tilde{\mathbf{x}}^i) + \beta_k \mathbf{P}(\tilde{\mathbf{x}}^s) + \sum_{l=0}^{k-1} \gamma_k^l \mathbf{P}(\mathbf{z}_l) + \alpha_{2,s} (B-1) \mathbf{P}(\mathbf{z}_{k-1}) + \alpha_{2,s} \mathbf{P}(\tilde{\mathbf{z}}_k) \\
= & (1 - \alpha_{2,s}) \mathbf{F}(\mathbf{y}_k) + \alpha_{3,s} \left\{ \frac{1}{2L_Q} \|\nabla \mathbf{F}(\mathbf{y}_k) - \mathbf{v}_k\|^2 + \langle \nabla \mathbf{F}(\mathbf{y}_k), \tilde{\mathbf{x}} - \mathbf{y}_k \rangle \right\} \\
& + \alpha_{2,s} (\mathbf{F}(\mathbf{y}_k) + \langle \mathbf{v}_k, \tilde{\mathbf{z}}_k - \mathbf{y}_k \rangle) + \frac{\bar{L}_s \alpha_{2,s} B}{2} \|\tilde{\mathbf{z}}_k - \mathbf{z}_{k-1}\|^2 + \mathbf{P}(\tilde{\mathbf{z}}_k) \\
& + \sum_{i=0}^{s-1} \lambda_k^i \mathbf{P}(\tilde{\mathbf{x}}^i) + \beta_k \mathbf{P}(\tilde{\mathbf{x}}^s) + \sum_{l=0}^{k-1} \gamma_k^l \mathbf{P}(\mathbf{z}_l) + \alpha_{2,s} (B-1) \mathbf{P}(\mathbf{z}_{k-1}) \\
& + \alpha_{2,s} \langle \mathbf{v}_k, \mathbf{y}_k - \mathbf{z}_{k-1} \rangle - \alpha_{3,s} \langle \nabla \mathbf{F}(\mathbf{y}_k), \tilde{\mathbf{x}} - \mathbf{y}_k \rangle \\
\leq & (1 - \alpha_{2,s}) \mathbf{F}(\mathbf{y}_k) + \alpha_{3,s} \left\{ \frac{1}{2L_Q} \|\nabla \mathbf{F}(\mathbf{y}_k) - \mathbf{v}_k\|^2 + \langle \nabla \mathbf{F}(\mathbf{y}_k), \tilde{\mathbf{x}} - \mathbf{y}_k \rangle \right\} \\
& + \alpha_{2,s} (\mathbf{F}(\mathbf{y}_k) + \langle \mathbf{v}_k, \mathbf{x}^* - \mathbf{y}_k \rangle) + \mathbf{P}(\mathbf{x}^*) + \frac{\bar{L}_s \alpha_{2,s} m}{2} (\|\mathbf{x}^* - \mathbf{z}_{k-1}\|^2 - \|\mathbf{x}^* - \tilde{\mathbf{z}}_k\|^2) \\
& + \sum_{i=0}^{s-1} \lambda_k^i \mathbf{P}(\tilde{\mathbf{x}}^i) + \beta_k \mathbf{P}(\tilde{\mathbf{x}}^s) + \sum_{l=0}^{k-1} \gamma_k^l \mathbf{P}(\mathbf{z}_l) + \alpha_{2,s} (B-1) \mathbf{P}(\mathbf{z}_{k-1}) \\
& + \alpha_{2,s} \langle \mathbf{v}_k, \mathbf{y}_k - \mathbf{z}_{k-1} \rangle - \alpha_{3,s} \langle \nabla \mathbf{F}(\mathbf{y}_k), \tilde{\mathbf{x}} - \mathbf{y}_k \rangle
\end{aligned}$$

Take expectation with respect to i_k and rearrange terms.

$$\begin{aligned}
& \mathbb{E}_{l,i_k} \mathbf{F}(\mathbf{x}_k) + \hat{\mathbf{P}}(\mathbf{x}_k) \\
\leq & (1 - \alpha_{2,s} - \alpha_{3,s}) \mathbf{F}(\mathbf{y}_k) + \alpha_{3,s} \mathbf{F}(\tilde{\mathbf{x}}^s) \\
& + \alpha_{2,s} (\mathbf{F}(\mathbf{y}_k) + \langle \nabla \mathbf{F}(\mathbf{y}_k), \mathbf{x}^* - \mathbf{y}_k \rangle) + \mathbf{P}(\mathbf{x}^*) + \frac{\bar{L}_s \alpha_{2,s} B}{2} (\|\mathbf{x}^* - \mathbf{z}_{k-1}\|^2 - \mathbb{E}_{i_k} \|\mathbf{x}^* - \tilde{\mathbf{z}}_k\|^2) \\
& + \sum_{i=0}^{s-1} \lambda_k^i \mathbf{P}(\tilde{\mathbf{x}}^i) + \beta_k \mathbf{P}(\tilde{\mathbf{x}}) + \sum_{l=0}^{k-1} \gamma_k^l \mathbf{P}(\mathbf{z}_l) + \alpha_{2,s} (B-1) \mathbf{P}(\mathbf{z}_{k-1}) \\
& + \alpha_{2,s} \langle \nabla \mathbf{F}(\mathbf{y}_k), \mathbf{y}_k - \mathbf{z}_{k-1} \rangle - \alpha_{3,s} \langle \nabla \mathbf{F}(\mathbf{y}_k), \tilde{\mathbf{x}} - \mathbf{y}_k \rangle \\
\leq & (1 - \alpha_{2,s} - \alpha_{3,s}) \mathbf{F}(\mathbf{y}_k) + \alpha_{3,s} \mathbf{F}(\tilde{\mathbf{x}}) \\
& + \alpha_{2,s} (\mathbf{F}(\mathbf{y}_k) + \langle \nabla \mathbf{F}(\mathbf{y}_k), \mathbf{x}^* - \mathbf{y}_k \rangle) + \mathbf{P}(\mathbf{x}^*) + \frac{\bar{L}_s \alpha_{2,s} B}{2} (\|\mathbf{x}^* - \mathbf{z}_{k-1}\|^2 - \mathbb{E}_{i_k} \|\mathbf{x}^* - \tilde{\mathbf{z}}_k\|^2) \\
& + \sum_{i=0}^{s-1} \lambda_k^i \mathbf{P}(\tilde{\mathbf{x}}^i) + \beta_k \mathbf{P}(\tilde{\mathbf{x}}) + \sum_{l=0}^{k-1} \gamma_k^l \mathbf{P}(\mathbf{z}_l) + \alpha_2 (B-1) \mathbf{P}(\mathbf{z}_{k-1}) + \alpha_{1,s} \langle \nabla \mathbf{F}(\mathbf{y}_k), \mathbf{x}_{k-1} - \mathbf{y}_k \rangle \\
\leq & \alpha_{3,s} (\mathbf{F}(\tilde{\mathbf{x}}) + \mathbf{P}(\tilde{\mathbf{x}})) + \alpha_{2,s} (\mathbf{F}(\mathbf{x}^*) + \mathbf{P}(\mathbf{x}^*)) + \frac{\bar{L}_s \alpha_{2,s} B}{2} (\|\mathbf{x}^* - \mathbf{z}_{k-1}\|^2 - \mathbb{E}_{i_k} \|\mathbf{x}^* - \tilde{\mathbf{z}}_k\|^2) \\
& + \alpha_{1,s} \sum_{i=0}^{s-1} \lambda_{k-1}^i \mathbf{P}(\tilde{\mathbf{x}}^i) + \alpha_{1,s} \beta_{k-1} \mathbf{P}(\tilde{\mathbf{x}}) + \alpha_{1,s} \sum_{l=0}^{k-1} \gamma_{k-1}^l \mathbf{P}(\mathbf{z}_l) + \alpha_{1,s} \mathbf{F}(\mathbf{x}_{k-1}) \\
= & \alpha_{3,s} (\mathbf{F}(\tilde{\mathbf{x}}) + \mathbf{P}(\tilde{\mathbf{x}})) + \alpha_{2,s} (\mathbf{F}(\mathbf{x}^*) + \mathbf{P}(\mathbf{x}^*)) + \alpha_{1,s} (\mathbf{F}(\mathbf{x}_{k-1}) + \hat{\mathbf{P}}(\mathbf{x}_{k-1})) \\
& + \frac{\bar{L}_s \alpha_{2,s} B^2}{2} (\|\mathbf{x}^* - \mathbf{z}_{k-1}\|^2 - \mathbb{E}_{l,i_k} \|\mathbf{x}^* - \mathbf{z}_k\|^2)
\end{aligned}$$

Subtract $\mathbf{F}(\mathbf{x}^*) + \mathbf{P}(\mathbf{x}^*)$ from both sides and use the fact that $\alpha_{1,s} + \alpha_{2,s} + \alpha_{3,s} = 1$, we have

$$\begin{aligned}
& \mathbb{E}_{l,i_k} \mathbf{f}^{\hat{\mathbf{P}}}(\mathbf{x}_k) - \mathbf{f}^{\mathbf{P}}(\mathbf{x}^*) \\
\leq & \alpha_{3,s} (\mathbf{f}^{\mathbf{P}}(\tilde{\mathbf{x}}) - \mathbf{f}^{\mathbf{P}}(\mathbf{x}^*)) + \alpha_{1,s} (\mathbf{f}^{\hat{\mathbf{P}}}(\mathbf{x}_{k-1}) - \mathbf{f}^{\mathbf{P}}(\mathbf{x}^*)) \\
& + \frac{\bar{L}_s \alpha_{2,s} B^2}{2} (\|\mathbf{x}^* - \mathbf{z}_{k-1}\|^2 - \mathbb{E}_{k,i_k} \|\mathbf{x}^* - \mathbf{z}_k\|^2)
\end{aligned}$$

Define $\hat{d}_k \stackrel{\text{def}}{=} \mathbf{f}^{\hat{\mathbf{P}}}(\mathbf{x}_k) - \mathbf{f}^{\mathbf{P}}(\mathbf{x}^*)$ and $\tilde{d} \stackrel{\text{def}}{=} \mathbf{f}^{\mathbf{P}}(\tilde{\mathbf{x}}) - \mathbf{f}^{\mathbf{P}}(\mathbf{x}^*)$, we have

$$\frac{1}{\alpha_{2,s}^2} \mathbb{E}_{k,i_k} \hat{d}_k \leq \frac{\alpha_{1,s}}{\alpha_{2,s}^2} \hat{d}_{k-1} + \frac{\alpha_{3,s}}{\alpha_{2,s}^2} \tilde{d} + \frac{\bar{L}_s B^2}{2} (\|\mathbf{x}^* - \mathbf{z}_{k-1}\|^2 - \mathbb{E}_{k,i_k} \|\mathbf{x}^* - \mathbf{z}_k\|^2) \quad (21)$$

Summing from $k = sm + 1$ to $(s+1)m$, we get

$$\frac{1}{\alpha_{2,s}^2} \sum_{j=1}^m \hat{d}_{j,s} \leq \frac{\alpha_{1,s}}{\alpha_{2,s}^2} \sum_{j=0}^{m-1} \hat{d}_{j,s} + \frac{\alpha_{3,s}}{\alpha_{2,s}^2} m \tilde{d} + \frac{\bar{L}_s B^2}{2} \{\|\mathbf{x}^* - \mathbf{z}_{0,s}\|^2 - \|\mathbf{x}^* - \mathbf{z}_{m,s}\|^2\}. \quad (22)$$

By rearranging terms, we have

$$\frac{\alpha_{1,s}}{\alpha_{2,s}^2} \hat{d}_{m,s} + \frac{1 - \alpha_{1,s}}{\alpha_{2,s}^2} \sum_{j=1}^m \hat{d}_{j,s} \leq \frac{\alpha_{1,s}}{\alpha_{2,s}^2} \hat{d}_{0,s} + \frac{\alpha_{3,s}}{\alpha_{2,s}^2} m \tilde{d} + \frac{\bar{L}_s B^2}{2} \{\|\mathbf{x}^* - \mathbf{z}_{0,s}\|^2 - \|\mathbf{x}^* - \mathbf{z}_{m,s}\|^2\}. \quad (23)$$

Using the fact that $\frac{1-\alpha_{1,s}}{\alpha_{2,s}^2} = \frac{\alpha_{3,s+1}}{\alpha_{2,s+1}^2}$, $\frac{1}{\alpha_{2,s}^2} = \frac{1-\alpha_{2,s+1}}{\alpha_{2,s+1}^2}$, we have $\frac{\alpha_{1,s}}{\alpha_{2,s}^2} = \frac{\alpha_{1,s+1}}{\alpha_{2,s+1}^2}$. From the definition of $\tilde{\mathbf{x}}^s$, we have

$$m\tilde{d}_{s+1} \leq \sum_{j=1}^m d_{j,s} \leq \sum_{j=1}^m \hat{d}_{j,s}, \hat{d}_{0,s} = \hat{d}_{m,s-1}, \mathbf{z}_{m,s-1} = \mathbf{z}_{0,s} \quad (24)$$

Additionally, using $\bar{L}_{s+1} \leq \bar{L}_s$, we have the following inequality

$$\begin{aligned} & \frac{\alpha_{1,s+1}}{\alpha_{2,s+1}^2} \hat{d}_{0,s+1} + \frac{\alpha_{3,s+1}}{\alpha_{2,s+1}^2} m\tilde{d}_{s+1} + \frac{\bar{L}_{s+1}B^2}{2} \|\mathbf{x}^* - \mathbf{z}_{0,s+1}\|^2 \\ & \leq \frac{\alpha_{1,s}}{\alpha_{2,s}^2} \hat{d}_{0,s} + \frac{\alpha_{3,s}}{\alpha_{2,s}^2} m\tilde{d}_s + \frac{\bar{L}_s B^2}{2} \|\mathbf{x}^* - \mathbf{z}_{0,s}\|^2 \end{aligned} \quad (25)$$

$$\tilde{d}_{s+1} \leq \frac{\alpha_{2,s+1}^2}{\alpha_{3,s+1}} \left(\frac{\alpha_{1,0}}{\alpha_{2,0}^2} \frac{d_0}{m} + \frac{\alpha_{3,0}}{\alpha_{2,0}^2} d_0 + \frac{\bar{L}_0 B^2}{2m} \|\mathbf{x}^* - \mathbf{z}_0\|^2 \right) \quad (26)$$

□

The non-proximal setting is special case of Theorem 2, and can be obtain by setting $\mathbf{P}(\mathbf{x}) = 0$ and remove the initialization constraints $\alpha_{2,0} = \alpha_{3,0} = 1/2B$.